Biomedicine & Pharmacotherapy 174 (2024) 116539

Contents lists available at ScienceDirect

Biomedicine & Pharmacotherapy

journal homepage: www.elsevier.com/locate/biopha

The effect of calpain inhibitor-I on copper oxide nanoparticle-induced damage and cerebral ischemia-reperfusion in a rat model

Hadi Karimkhani [a,e,*], Paria Shojaolsadati [b], Türkan Yiğitbaşı [c], Bircan Kolbası [d], Neslin Emekli [c]

[a] Department of Biochemistry, School of Medicine, Istanbul Okan University, Istanbul, Turkey
[b] Department of Anatomy, School of Medicine, Yeditepe University, Istanbul, Turkey
[c] Department of Biochemistry, School of Medicine, Istanbul Medipol University, Istanbul, Turkey
[d] Department of Histology and Embryology, School of Medicine, Istanbul Medipol University, Istanbul, Turkey
[e] Department of Stem Cell, School of Medicine, Eskisehir Osmangazi University, Eskisehir, Turkey

ARTICLE INFO

Keywords:
Copper oxide nanoparticle (CuO-NP)
Brain ischemia-reperfusion (I/R)
Cerebral ischemia-reperfusion (I/R)
Calpain inhibitor
Anti-apoptotic treatment
Rat model

ABSTRACT

This study aimed to investigate the effects of the calpain inhibitor N-Acetyl-Leu-Leu-norleucinal (ALLN) on neuroapoptotic cell damage caused by Copper Oxide Nanoparticles (CuO-NP) and exacerbation of damage through brain ischemia/reperfusion (I/R) in a rat model. Male Wistar Albino rats (n=80) were divided into eight groups: Control, I/R, CuO-NP, CuO-NP+I/R, I/R+ALLN, CuO-NP+ALLN, CuO-NP+I/R+ALLN, and DMSO. Biochemical markers (MBP, S100B, NEFL, NSE, BCL-2, Cyt-C, Calpain, TNF-α, Caspase-3, MDA, and CAT) were measured in serum and brain tissue samples. Histological examinations (H&E staining), DNA fragmentation analysis (TUNEL) were performed, along with Caspase-3 assessment. The ALLN-treated groups exhibited significant improvements in biochemical markers and a remarkable reduction in apoptosis compared to the damaged groups (CuO-NP and I/R). H&E and Caspase-3 staining revealed damage-related morphological changes and reduced apoptosis in the ALLN-treated group. However, no differences were observed among the groups with TUNEL staining. The findings suggest that ALLN, as a calpain inhibitor, has potential implications for anti-apoptotic treatment, specifically in mitigating neuroapoptotic cell damage caused by CuO-NP and I/R.

1. Introduction

The human brain is a metabolically active organ that is highly sensitive to disruptions in blood flow. Cerebral ischemia occurs when cerebral blood flow falls below a critical threshold, resulting in general or regional brain damage [1,2]. During the ischemic phase, damage to oxygen-dependent cells takes precedence [2,3]. When blood flow is restored, ischemia/reperfusion injury occurs [4]. Reperfusion introduces a sudden influx of oxygen, paradoxically increasing oxidative stress and triggering additional inflammatory responses, leading to cellular and tissue damage [5]. Numerous pharmacological strategies have been suggested to prevent ischemia/reperfusion injury. While the brain has defense mechanisms against ischemia, the impact of reactive oxygen species can cause cellular events and mitochondrial dysfunction [6]. Various animal models, such as global and focal ischemia, are used to study ischemia/reperfusion injury [7]. Global ischemia reduces blood flow throughout the brain, while focal ischemia affects specific areas. Both occlusion models induce global ischemia in rats [1]. Damage raises the amount inside cells, which turns on metabotropic glutamate receptors through G-proteins and lets calcium out through the IP3 system [8].

Copper nanoparticles (Cu-NPs) are extensively utilized in various industries due to their exceptional properties. With applications ranging from food packaging, where they contribute to prolonging the shelf life of food products and inhibiting the growth of bacteria and mold, to agriculture, where they effectively assist in controlling plant diseases and pests, Cu-NPs have proven their versatility and efficacy. Furthermore, the use of copper nanoparticles (Cu-NPs) extends to cosmetic products, particularly sunscreens, due to their ability to safeguard against skin infections and provide effective shielding against harmful solar radiation. As a result, CuO-NPs have gained significant popularity across multiple industries [9–12]. However, it is imperative to consider the potential risks associated with their usage. The concern lies in the ability of these nanoparticles to enter the food chain, with their long-term effects on human health yet to be fully understood. Furthermore, the environmental implications of Cu-NPs should not be

* Corresponding author at: Department of Biochemistry, School of Medicine, Istanbul Okan University, Istanbul, Turkey.
E-mail address: drhadi.h@gmail.com (H. Karimkhani).

https://doi.org/10.1016/j.biopha.2024.116539
Received 7 December 2023; Received in revised form 18 March 2024; Accepted 29 March 2024
Available online 13 April 2024

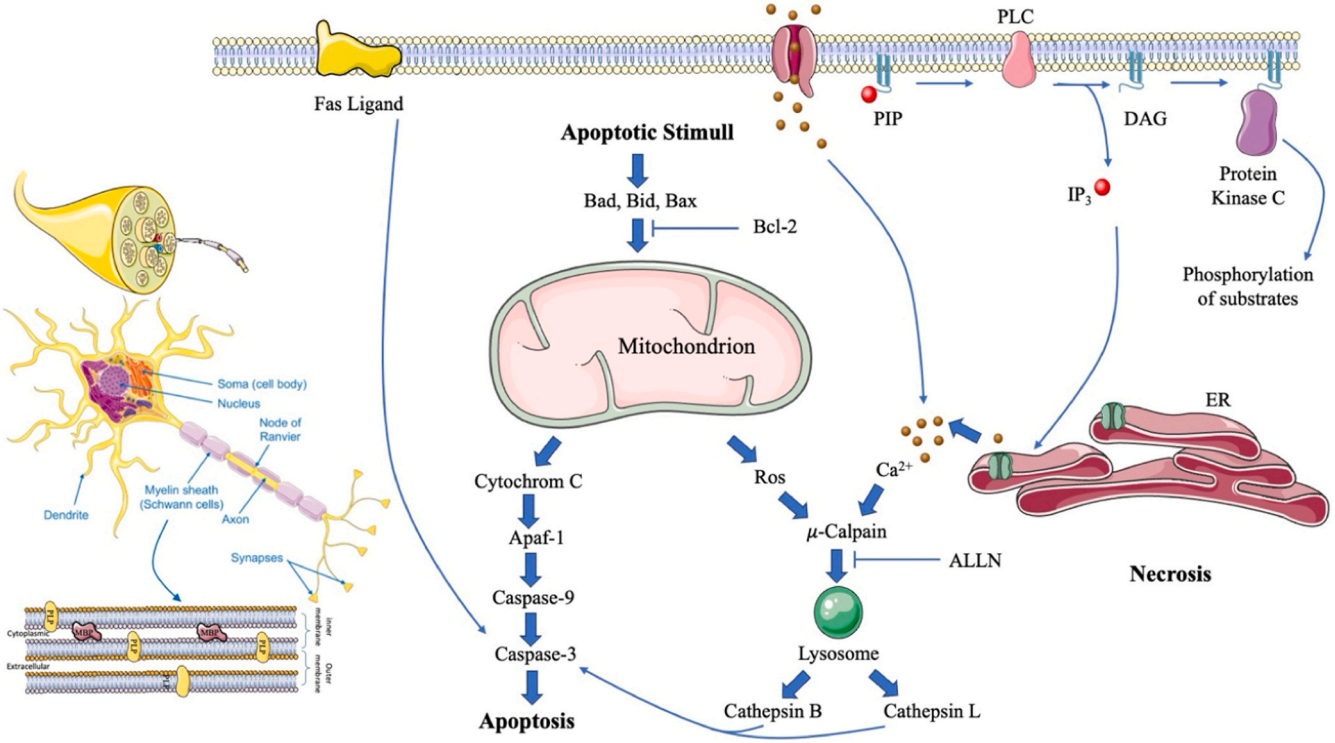

Fig. 1. Graphical Abstract.

overlooked, as they may have adverse effects on ecosystems. In addition to other impacts, Cu-NPs are harmful due to their rapid consumption of hydrogen ions, leading to the formation of highly reactive copper ions. These characteristics contribute to their potential to harm the environment and enter the human body through wastewater and other waste products [13]. Moreover, both Cu and CuO nanoparticles have demonstrated higher toxicity compared to many other metal and metal oxide nanoparticles [14]. In conclusion, while Cu-NPs offer various benefits in terms of their properties and applications, it is crucial to thoroughly evaluate the potential risks and drawbacks associated with their usage. A comprehensive and balanced assessment is necessary to ensure their safe and responsible utilization, considering the potential environmental and health concerns that may arise.

Calpain's function in neuronal death and nerve injury has been the subject of numerous research investigations. Calpains are currently known to be a class of enzymes comprising fifteen members, thanks to the discovery of distinct isoforms. Two types of calpain, Calpain- I (μ-calpain) and Calpain-II (m-calpain), are found in all tissues and organs, including the brain [15]. Calpain-I and -II require different levels of calcium for activation. Calpain-I requires micromolar concentrations of calcium for activation, whereas Calpain-II requires millimolar levels of it [15]. Calpain-I is involved in controlling dendrite structure and localized protein synthesis through the cleavage of many critical proteins. Additionally, calpain has been shown to cleave β-catenin, introducing an effective region that modulates transcriptional activity [15–17].

Calpain overactivity indirectly leads to lysosomal permeabilization, resulting in the production of cathepsin-B, Which is this cysteine protease exacerbates lysosomal membrane rupture and induces mitochondrial damage, leading to the release of pro-apoptotic proteins such as Cytochrome C, Caspase-9, and Caspase-3 [18,19]. In the reperfusion process, blood flow to the brain is restored. This damages the brain in several ways, including through neutrophil migration, higher ROS levels, cerebral edema, and excessive blood loss. The increased ROS levels cause damage to intracellular proteins and DNA through various pathways that trigger oxidation and cell death [1]. While ROS are formed during normal metabolic processes and play a role in critical physiological mechanisms, they can harm cells when produced in large amounts due to oxidative stress [6].

Calpains are proteases that work with the cytoskeleton and signal transduction. They are involved in many physiological and pathophysiological processes, such as controlling the cell cycle, apoptosis, inflammation, ischemia, muscular dystrophies, cataract genesis, Alzheimer's disease, and Parkinson's disease. It has been established that activated calpains cause damage to lysosomal membranes during necrotic cell death. The initial consequence of ischemic events is the incorporation of calpains into lysosomal membranes, leading to cell lysis [17,18,20]. An increased level of intracellular Ca^{2+} disrupts the function of the mitochondrial membrane, resulting in autolysis and cell death. This process is accompanied by vesiculation of the endoplasmic reticulum, lysosomal swelling, loss of enzymes and proteins, disintegration of cellular compartments, and break down of membrane integrity [19,21,22]. In specific investigations, a single-dose calpain inhibitor has been shown to improve the microenvironment of brain damage by suppressing inflammation and reducing apoptosis, thereby decreasing the infarct area [23].

The study used an ischemia-reperfusion (I/R) model to damage the brain, damage, and CuO-NP was used to make damage worse and boost the effects of ischemia-reperfusion. This approach aimed to evaluate the protective effect of a calpain inhibitor, such as ALLN, more effectively. In summary, CuO-NP was used to exacerbate brain damage in the ischemia-reperfusion model, enabling a more comprehensive understanding and assessment of the protective effects of ALLN.

The inhibition of calpain activation, which plays a role in tissue damage, has gained increasing importance in recent years. Numerous research studies have explored the involvement of calpain in various physiological and pathological conditions, including neurodegenerative diseases, cardiovascular disorders, and cancer. Calpain inhibitors have been extensively investigated for their potential therapeutic applications in these conditions. Several calpain inhibitors have been identified and

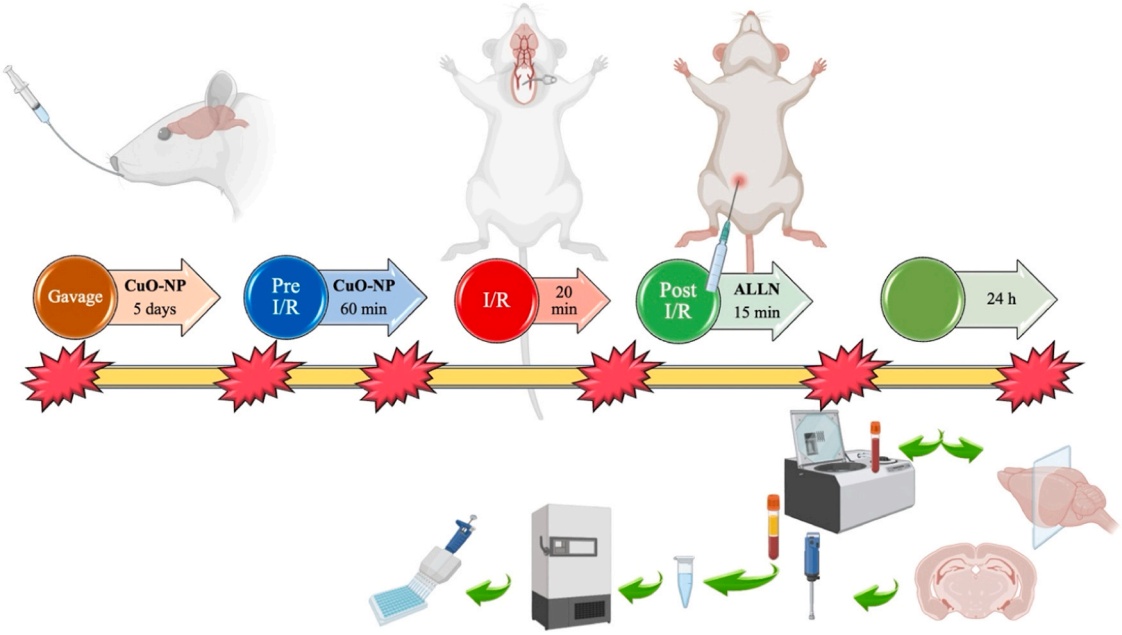

Fig. 2. Schematic chart of the Neurological Calpain Inhibitor-I (ALLN) on CuO-NP Induced and Brain Ischemia-Reperfusion.

tested for their ability to prevent or reduce calpain-mediated cellular damage and disease progression. Therefore, many research studies have investigated the effects of calpain inhibitors, including ALLN, in various cellular and animal models. Although a considerable amount of research has been conducted on this topic, further investigations are necessary to fully comprehend the mechanisms and potential therapeutic applications of calpain inhibition. There are more than a dozen known calpain inhibitors, and in this study, a calpain inhibitor called ALLN was used (Fig. 1).

2. Materials and methods

2.1. Materials and chemicals

All chemicals used in the study, including N-Acetyl-Leu-Leu-Norleucinal (ALLN) and CuO-NP nanoparticles, were purchased from commercial suppliers such as Sigma-Aldrich and Merck (St. Louis, MO, USA). These chemicals were either of analytical grade or the highest available grade and were utilized without any additional purification steps. Throughout the experiments, ultra-pure water was consistently employed.

2.2. Animals

250–300 g Wistar Albino male rats aged 6–8 weeks were used in the experiments. The rats were kept in standard animal care cages with a 12-hour day/night cycle, maintained at a constant temperature of 22±3°C and a constant humidity of 55±5%. The rats were placed in separate cages and acclimated to laboratory conditions for two days before starting the experiments. The animal training and treatments were conducted in accordance with authorized institutional animal care standards and aligned with the Istanbul Medipol University for Laboratory Animals. The Istanbul Institutional Animal Ethics Committee (no. 38828770–604.01.01-E.15939) at the University of Istanbul Medipol approved all animal procedures used in this study.

2.3. Experimental design and treatment schedule

The above steps were applied to the determined groups. The groups are explained according to the numbers below, and the experimental phase is shown on the chart (Fig. 2). A total of 80 rats were randomly divided into eight groups:

A. Control group (n=10): The rats were given 2 mL of physiological saline (SF) by gavage for five days.

B. I/R Group (n=10): The rats in this group were given 2 mL of saline by gavage for five days, and 60 minutes after the last day, an I/R damage model was induced.

C. CuO-NP Group (n=10): The rats in this group were given 200 mg/kg copper oxide nanoparticles by gavage for five days.

D. CuO-NP+I/R Group (n=10): The rats in this group were given 200 mg/kg copper oxide nanoparticles by gavage for five days. An I/R model was induced 60 minutes after the last day.

E. I/R+ALLN Group (n=10): The rats in this group were given 2 mL of saline by gavage for five days. After 60 minutes, an I/R model was induced, and 20 mg/kg of the calpain inhibitor ALLN was given 15 minutes later.

F. CuO-NP+ALLN Group (n=10): The rats in this group were given 200 mg/kg copper oxide nanoparticles by gavage for five days, and 15 minutes after the last day, 20 mg/kg of the calpain inhibitor ALLN was given.

G. CuO-NP+I/R+ALLN Group (n=10): The rats in this group were given 200 mg/kg copper oxide nanoparticles by gavage for five days. An I/R model was induced 60 minutes after the last day, and 15 minutes later, 20 mg/kg of the calpain inhibitor ALLN was given.

H. Solvent group (n=10): The rats in this group were given 2 mL of physiological saline by gavage for five days. After 60 minutes, an I/R model was induced, and 15 minutes later, a DMSO solution containing the dissolved calpain inhibitor was administered.

- Histological and biochemical parameters were evaluated using tissue and serum samples obtained from 80 rats (n=10 in each group).
- Animal experiments were conducted in groups, with each group lasting approximately 7–10 days.

After 24 hours of the experiment, following anesthesia, blood was collected intracardially. The collected blood samples were then centrifuged, and the resulting serum samples were stored at −80 °C. Subsequently, the rats were decapitated, and the brain tissues were frozen on dry ice and kept at −80 °C until the study. For histological studies, tissue sections were obtained using a cryostat, and these sections were fixed. Following fixation, the sections underwent staining and immunohistochemical examination.

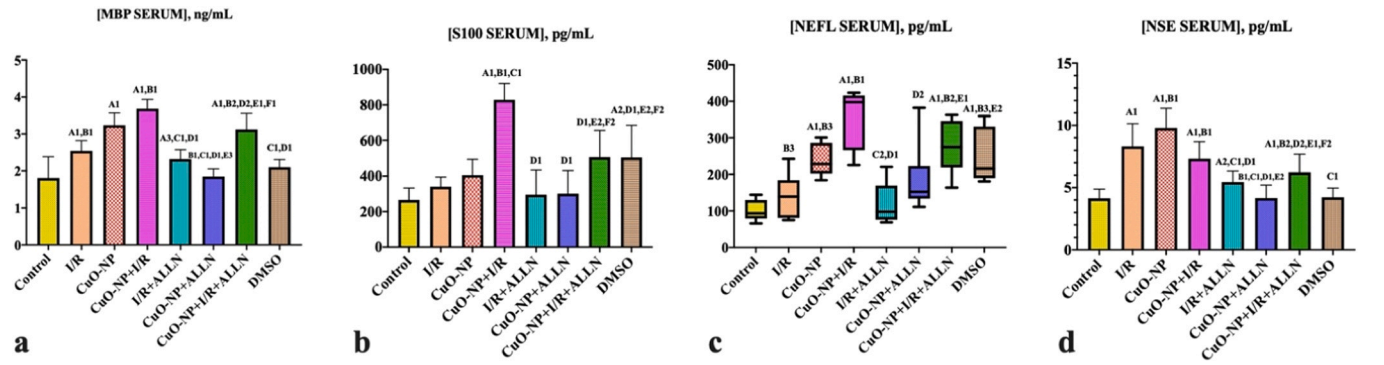

Fig. 3. Biochemical Parameters Measured in Serum. This figure presents the levels of a.MBP, b.S100, c.NEFL, and d.NSE in different groups (n=10). The data are presented as mean ± S.D. in each group. Significant differences ($p<0.05$) were observed between the Control and I/R, CuO-NP, CuO-NP+I/R, I/R+ALLN, and CuO-NP+ALLN groups, as indicated by the corresponding letters (A-F) and numbers (1−3). Specifically, the numbers 1, 2, and 3 indicate p-values of less than 0.001, 0.01, and 0.05, respectively (n=10).

2.4. Nanoparticle infusion

The rats in the study were administered orally 200 mg/kg body weight of CuO-NP nanoparticles (Sigma-544868) by gavage. This procedure was applied once a day for five days in groups 3, 4, 6 and 7 [24].

2.5. Ischemia/Reperfusion (I/R) model

The rats in groups 2, 4, 6, and 7 were allowed to drink water freely during the period, and the operation was performed. Singh and Chopra had previously described a model of transient global cerebral ischemia. After 20 minutes, the clamp was released, and blood flow was re-initiated before closing it with the incision. Saline (5 mL) was injected intraperitoneally at 37°C to prevent fluid loss during surgery [25] (Fig. 2).

2.6. ALLN application

Rats in groups 4, 5, and 6 were intraperitoneally injected with 20 mg/kg of ALLN (Merck) 15 minutes after I/R. ALLN was dissolved in 2 mL of dimethyl sulfoxide (DMSO), and the solvent group received only 2 mL of DMSO intraperitoneally [26,27].

2.7. Parameters measured in serum

The serum levels of Rat Myelin Basic Protein (MBP) (E-EL-R0642), Rat S100B (S100 Calcium Binding Protein B) (E-EL-R0868), Rat Neurofilament, Light Polypeptide (NEFL) (E-EL-R2536), and Rat Neuron Specific Enolase (NSE) (E-EL-R0058) were measured using ELISA assays.

2.8. Parameters measured in brain tissue

First, the brain tissues were homogenized. The brain tissues were removed, weighed, and stored at −80°C until the study. The tissues were thawed and then homogenized by adding a 1:10 phosphate buffer solution (PBS) (pH 7.2). The resulting homogenates were then centrifuged at 5000×g for 10 minutes at +4°C. The supernatants obtained were used for measurement. The levels of B-cell Lymphoma/Leukemia 2 (Bcl-2) (E-EL-R0096), Rat Cytochrome C (Cyt-C) (E-EL-R0160), Rat Calpain I (CAPN1) (E-EL-R2537), Tumor Necrosis Factor Alpha (TNF-α) (E-EL-R0019), and Caspase-3 (CASP3) (E-EL-R2537) in brain tissue were measured using an ELISA assay.

The levels of malondialdehyde (MDA) in brain tissue were measured by reaction with thiobarbituric acid (TBA) to form a colored product. Samples were treated with mixtures containing SDS, acetate buffer, TBA, and distilled water. After incubation and centrifugation, the resulting supernatant was used for measurement. The absorbance values of the samples were measured at 532 nm, and the concentrations were calculated using a standard curve. The total protein levels of the same homogenates were measured, and the MDA concentrations of the samples were normalized to the total protein. The results represent the tissue MDA levels in nmol/mg protein [28]. The measurement of catalase (CAT) levels in brain tissue involves the catalytic breakdown of H_2O_2. The rate of H_2O_2 decomposition by CAT was measured spectrophotometrically based on its absorption of light at 230 nm. The specific activity of catalase (U/mg protein) was calculated by dividing the catalase activity by the amount of protein [28]. The protein content of the homogenates obtained from brain tissue was measured using the Bradford method [28].

2.9. Histological findings in brain tissue

Brain tissue samples were collected and stored at −80°C for histological experiments until use. Subsequently, the tissue was sectioned into 17 μm-thick coronal sections using a cryostat (CM1950) (Leica, Wetzlar, Germany). These sections were then stained with hematoxylin-eosin (H&E) (Empire Genomics, BPK 4088–2) according to the manufacturer's instructions for light microscopy examination. For Caspase-3 immunofluorescence and method applications, the tissue sections were frozen and then fixed with 4% PFA at room temperature for 20 minutes. After fixation, sections were blocked with a blocking agent (10% normal goat serum, 3% bovine serum albumin, 0.1% sodium azide, and 1% Tween-20) for 1 hour at room temperature. Slides were incubated overnight at 4°C with the primary antibody anti-Caspase-3 (1:200, Abcam 13837) without washing. The following day, sections were washed with PBS and incubated at room temperature for an hour with goat anti-rabbit immunoglobulin G (IgG) H&L-Alexa Fluor 488 (1:500; ab 150077). A dye called DAPI (D1306, Thermo Scientific) was used to color the nuclei in TUNEL and caspase-3 immunofluorescence experiments. The images were captured using a confocal microscope LSM 780 (Carl Zeiss, Oberkochen, Germany). For TUNEL assays, sections were fixed with 4% PFA at room temperature for 20 minutes and then labeled with TUNEL (11684795910, F. Hoffmann-La Roche Ltd., Basel, Switzerland) according to the manufacturer's instructions.

2.10. Statistical analysis

Statistical analysis was performed using SPSS (Statistical Package for Social Sciences) Windows 26.0 software. The normality of the data distributions was assessed using the Kolmogorov-Smirnov and Shapiro-Wilk tests. For normally distributed data, group comparisons were performed using one-way ANOVA and Tukey HSD tests, and the results were presented as the mean ± standard deviation (SD). Non-normally

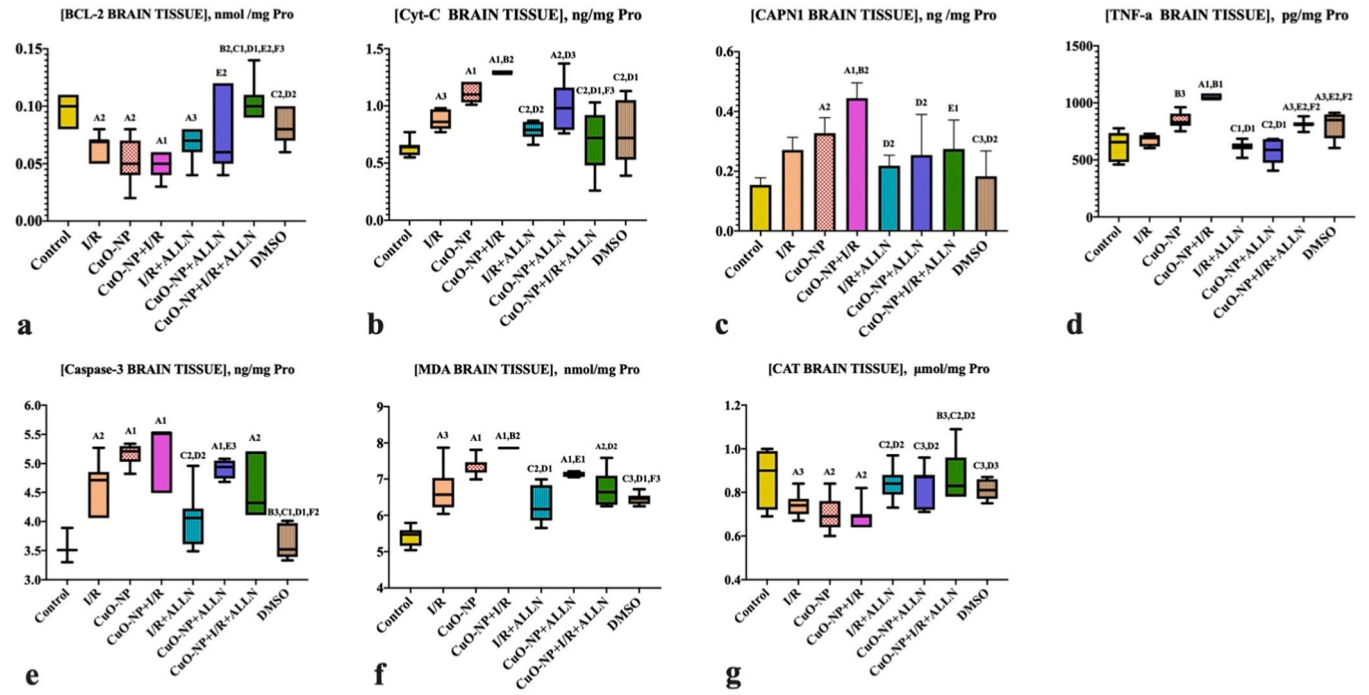

Fig. 4. Biochemical Parameters Measured in Brain Tissue. This figure presents the levels of a.BCL-2, b.Cyt-C, c.CAPN1, d.TNF-a, e.Caspase-3, f.MDA, and g.CAT in brain tissue samples different groups (n=10). The data are presented as mean ± S.D. in each group. Significant differences ($p<0.05$) were observed between the Control and I/R, CuO-NP, CuO-NP+I/R, I/R+ALLN, and CuO-NP+ALLN groups, as indicated by the corresponding letters (A-F) and numbers (1−3). Specifically, the numbers 1, 2, and 3 indicate p-values of less than 0.001, 0.01, and 0.05, respectively (n=7).

distributed data were analyzed using the Kruskal-Wallis test, and post-hoc multiple comparisons were conducted using the Tukey HSD test. The results were presented as the median, 25th percentile, and 75th percentile. Variable relationships were evaluated using Pearson and Spearman correlation tests. A p-value of less than 0.05 was considered statistically significant.

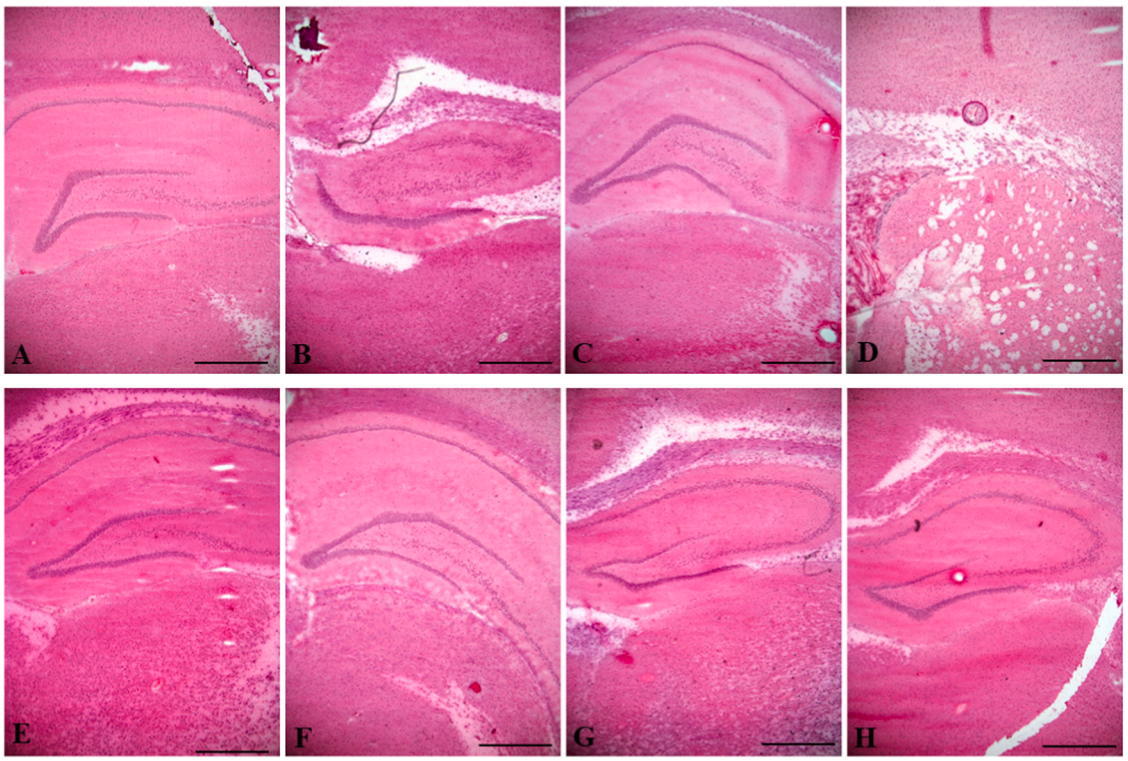

Fig. 5. Morphology of the CA3 region of the hippocampus was examined using Hematoxylin and Eosin (H&E) staining. Shows the morphological changes (indicated by black arrows) observed: A.Control group, B.I/R group, and C.CuO-NP+I/R+ALLN group (n=7).

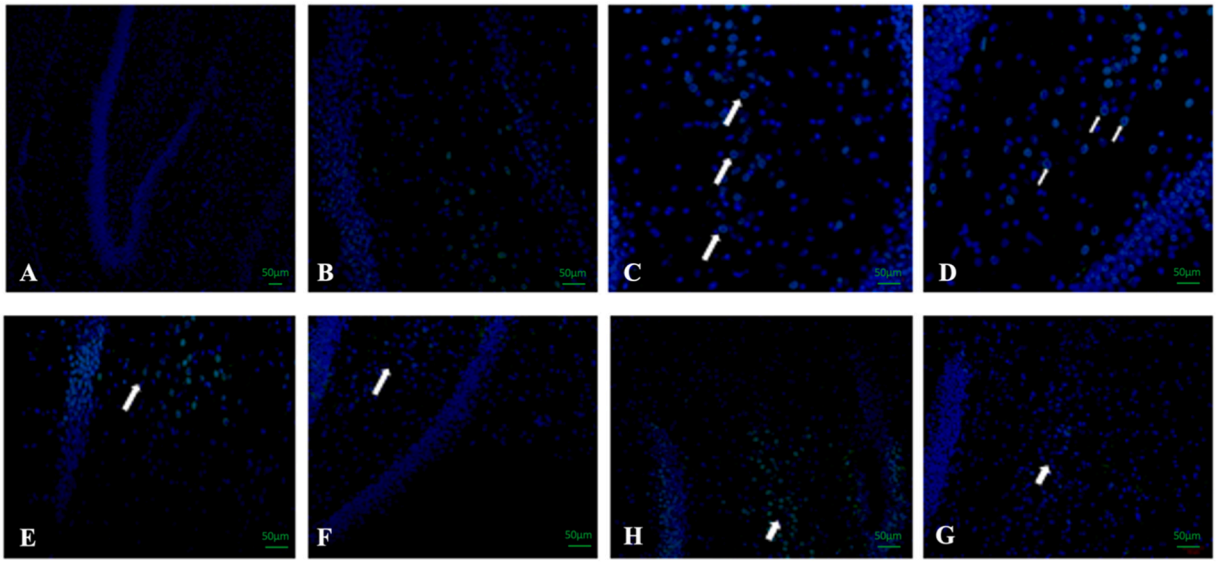

Fig. 6. Assessment of Apoptotic Cell Density using Caspase-3 Immunofluorescence Staining. The density of apoptotic cells was examined using Caspase-3 immunofluorescence staining. No apoptotic cells were observed in the Control and DMSO groups (A and B), while apoptotic cells were present in the CuO-NP (C), I/R (D), and CuO-NP+I/R (E) groups (indicated by white arrows). The CuO-NP+ALLN (F), I/R+ALLN (G), and CuO-NP+I/R+ALLN (H) groups showed a decrease in apoptotic cell density. The images were magnified at 20X for A-H (n=7). (B-H: include digital zoom.).

3. Results

3.1. Biochemical parameters measured in serum

The study's findings demonstrated that a rat model with CuO-NP and I/R damage could receive ALLN, a calpain inhibitor. The levels of MBP, S100, NEFL, and NSE in the serum of the rats were measured, and their statistical analysis of these measurements is presented (Fig. 3). When comparing the levels of MBP, S100, NEFL, and NSE between the treatment groups (I/R+ALLN, CuO-NP+ALLN, and CuO-NP+I/R+ALLN), and the damaged groups (I/R, CuO-NP, and CuO-NP+I/R), a decrease was observed in the all treatment group as a whole. This decrease showed statistically significant differences between the MBP and NSE markers ($p>0.5$, $p<0.001$, $p<0.01$). Regarding S100 levels, a significant decrease was observed only between the CuO-NP+I/R+ALLN and CuO-NP+I/R groups ($p<0.001$). However, it was determined that the reduction in NEFL levels did not show a statistically significant difference among any treatment group ($p>0.5$).

3.2. Biochemical parameters measured in brain tissue

Furthermore, the levels of Bcl-2, Cyt-C, CAPN1, TNF-α, Caspase-3, MDA, and CAT in the brain tissue of the rats were also measured, and the results are presented (Fig. 4). The levels of Bcl-2 were compared

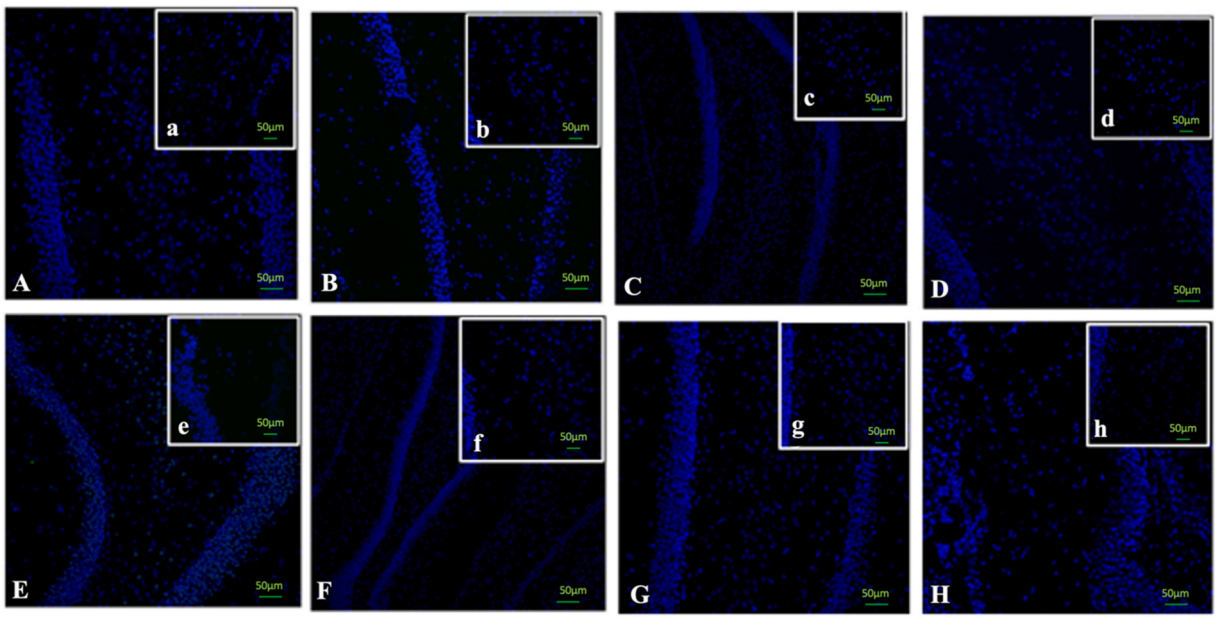

Fig. 7. Assessment of Apoptotic Cell Density using the TUNEL Method. The TUNEL method was used to assess apoptotic cell density. The Control and DMSO groups (A and B) showed no significant difference in apoptotic cell density compared to the CuO-NP (C), I/R (D), and CuO-NP+I/R groups (E). Similarly, there was no significant difference in apoptotic cell density observed between the treatment groups (CuO-NP+ALLN (F), I/R+ALLN (G), and CuO-NP+I/R+ALLN (H)) and the damaged or control groups. The images were magnified at 10X for A-H and 20X for a-h (n=7).

between the damaged groups (I/R, CuO-NP, and CuO-NP+I/R) and the treatment groups (I/R+ALLN, CuO-NP+ALLN, and CuO-NP+I/R+ALLN). There were statistically significant differences in the order of rise ($p>0.5$, $p>0.5$, $p<0.001$). The levels of Cyt-C, TNF-α, CAPN1, Caspase-3, MDA, and CAT showed statistically significant differences in the order of decrease when comparing the treatment groups to the damaged groups ($p>0.5$, $p>0.5$, $p<0.001$), ($p>0.5$, $p<0.01$, $p>0.5$), ($p>0.5$, $p>0.5$, $p>0.5$), ($p>0.5$, $p>0.5$, $p>0.5$), ($p>0.5$, $p>0.5$, $p<0.01$), ($p>0.5$, $p<0.5$, $p<0.01$). Only in the I/R+ALLN group were no statistically significant differences observed in any of the markers, but significant differences were observed in the CuO-NP+I/R+ALLN group compared to the overall damaged group.

3.3. Histopathological studies

The morphological examinations using hematoxylin and eosin (H&E) staining were conducted to observe the structural changes in the CA3 region of the hippocampus. According to the findings, the study investigated morphological alterations in the hippocampus. Light microscopy examinations revealed areas where cell organization was disrupted in the hippocampus belonging to the injury group. It was observed that the organization in the ALLN application was similar to the control group. These results suggest that ALLN may be effective in preserving hippocampal neurons and reversing the effects of damage (Fig. 5). The results of Caspase-3 immunofluorescence staining also provide noteworthy findings. In the control group, no Caspase-3-positive cells were observed. In the DMSO and injury groups, caspase-3 immune-positive cells were seen. However, in the ALLN treatment groups, a few Caspase-3-positive cells were seen (Fig. 6). On the other hand, evaluations of apoptotic cell density using the TUNEL method yielded different results. There was no significant difference in apoptotic cell density between the damage group, control group, and DMSO group, as well as the ALLN treatment groups. These results suggest that different apoptosis detection methods can influence the outcomes (Fig. 7).

4. Discussion

Irreversible brain cell damage resulting from I/R is one of the most critical health problems concerning mortality and morbidity. When reviewing the literature on the subject, it becomes evident that calpain inhibitor-I (ALLN) exhibits therapeutic effects on different damages. Brain ischemia injury and copper nanoparticle injury are two types of neurodegenerations that the calpain-I inhibitor could be used to treat. Investigating calpain inhibitors as a novel combination treatment technique to enhance the cellular effects of brain damage is worth considering [23]. In this study, we looked into the effects of calpain inhibitor-I (ALLN) on treating I/R and CuO-NP-related brain damage. We designed different experimental groups to reveal the effects of CuO-NP on the damage. We examined the damage mechanisms in groups exposed to CuO-NP, groups undergoing brain I/R, and groups of rats in which brain tissue was more damaged by exposure to both. One of the essential differences distinguishing I/R from other diseases is that it develops suddenly, and most deaths occur within the first few hours. For this reason, researchers conduct numerous studies on this subject to prevent I/R and reduce complications that may arise after I/R. Moreover, CuO-NP, widely used in the food and packaging industry, can also enter the body through different foods and cause toxic effects on the organs. Likewise, nanoparticles, substances used in different sectors, can quickly enter the body and cause toxic damage. Therefore, in this study, we investigated the effect of ALLN on more severe injuries caused by brain I/R after acute CuO-NP exposure. According to the biochemical criteria used to measure the damage caused within the brain tissues of rats, the effect of ALLN was found to be successful.

This is one step of the project that will develop new ways with calpain inhibitor-I to prevent brain damage caused by CuO-NP. The findings we have obtained through ELISA analysis suggest that ALLN can eliminate the adverse effects on the brain [26,27,29,30].

Mitochondria are crucial in maintaining cellular stability and initiating cell death pathways. To determine the optimal timing for administering ALLN to the experimental group, we focused on releasing the anti-apoptotic protein Bcl-2 from mitochondria. Previous studies found that administering ALLN after I/R helped increase Bcl-2 levels, thereby protecting brain cells from apoptosis. Ischemic and hypoxic damage trigger nervous system cell death by releasing cytokines and activating cell death receptors. Our study found apoptosis, damage to the mitochondria, release of cytochrome C into the cytoplasm, increased caspase, and nuclear condensation, which is similar to what other studies have found [31].

Our results show that inhibiting calpain is helpful in lowering TNF-α levels, which is an inflammatory marker, to stop brain cells from dying in rats that were given I/R and CuO-NP. Furthermore, our study supports the notion that ALLN has potent anti-inflammatory properties. These findings align with those of Das and Izumi colleagues, who have confirmed the critical role of inflammation in the development of neurodegenerative diseases. Our data emphasize the mechanisms by which ALLN can safeguard brain cells against these processes [31,32].

The results of our study show that I/R and CuO-NP exposure lowers Bcl-2 levels, which causes cell death signals to start earlier and more caspases to be activated. Calpain activation, which includes caspase-3 activation, has been observed to increase. Moreover, our results reveal that cytochrome c cleavage due to I/R and CuO-NP exposure causes an increase in Caspase-3 levels, which can be counteracted by ALLN treatment. These observations are consistent with the studies conducted by Das and Smith [29,31,33].

Our research showed that calpain inhibitors can reduce the severity of cell damage in I/R and CuO-NP models by preserving the axon-myelin structure and preventing axonal degradation, indicating that calpain inhibitor therapy may hold promise in the treatment of neurodegenerative diseases. In this study, ALLN treatment also helped protect brain cells by stopping calcineurin from taking part in the apoptotic process and reducing S100B levels. Interestingly, Berger and Donato et al. reported increased S100B levels in damage groups. To learn more about the intracellular signaling pathways involved in the survival-enhancing effects of ALLN, we investigated whether ALLN supports brain cells through intracellular signaling cascades. High intracellular Ca^{2+} and calpain activation levels can lead to apoptotic cell death through various mechanisms. Our finding that a calcineurin inhibitory mutant is malignant and suppresses apoptosis suggests that calcineurin is the primary mediator of apoptotic death signals [34–36].

Neurofilaments (NFs) are structural proteins that comprise the cytoskeleton of nerve cells' dendrites and axons. When an ischemic event occurs in the brain, NFs can become part of the cytoskeleton and cause mechanical damage to nervous tissue. However, if NFs continue dissociating, they can lead to neuronal death and dysfunction in the central nervous system. Research by Aronowski, Gresle, and Kobek has shown that changes in NFs also occur in axonal damage following traumatic brain injury. The results of our study support these findings, as we observed recovery in the groups treated with ALLN after I/R and CuO-NP exposure, which was indicated by a decrease in NF value [37–39].

After five days of exposure to CuO-NP, cell damage due to ROS takes place in brain cells. Malondialdehyde (MDA), one of the oxidant parameters that show damage in neurological disorders, increased, and a decrease in catalase (CAT), one of the antioxidant parameters, was observed. In our study, we found that the levels of MDA, an oxidant parameter that reflects damage in neurological disorders, rose, and the levels of CAT, an antioxidant parameter, declined in groups with brain damage. Our results indicate that in the treatment groups given ALLN, the values of MDA and CAT remained comparable to those of the control group [24,28,40].

Brain injury biomarkers, including NSE, S-100β, and MBP, have been

Table 1
Biochemical Parameters Measured in Serum. This table presents the levels of MBP, S100, NEFL, and NSE in serum markers from different groups (n = 10). The data are presented as mean ± S.D. in each group. Significant differences ($p<0.05$) were observed between the Control and I/R, CuO-NP, CuO-NP+I/R, I/R+ALLN, and CuO-NP+ALLN groups, as indicated by the corresponding letters (A-F) and numbers (1−3). Specifically, the numbers 1, 2, and 3 indicate p-values of less than 0.001, 0.01, and 0.05, respectively.

Groups	N	MBP (ng/mL /mg pro)	S100B (pg/mL /mg pro)	NEFL (pg/mL /mg pro)	NSE (pg/mL /mg pro)
Control	10	1.81±0.58	265.46±67.20	102±28	4.13±0.74
I/R	10	2.54±0.27$^{A1, B1}$	340.08±54.36	141±63^{B3}	8.32±1.81^{A1}
CuO-NP	10	3.24±0.33^{A1}	405.39±88.91	238±43^{A1,B3}	9.79±1.58$^{A1, B1}$
CuO-NP+I/R	10	3.68±0.25$^{A1, B1}$	828.93±91.48$^{A1, B1, C1}$	353±79$^{A1, B1}$	7.32±1.36$^{A1, B1}$
I/R+ALLN	10	2.32±0.25$^{A3, C1, D1}$	294.85±139^{D1}	119±53$^{C2, D1}$	5.45±0.88$^{A2, C1, D1}$
CuO-NP+ALLN	10	1.85±0.20$^{B1, C1, D1, E3}$	299.61±130.06^{D1}	185±81^{D2}	4.16±1.05$^{B1, C1, D1, E2}$
CuO-NP+I/R+ALLN	10	3.12±0.43$^{A1, B2, D2, E1, F1}$	507±149.42$^{A2, D1, E2, F2}$	278±69$^{A1, B2, E1}$	6.22±1.47$^{A1, B2, D2, E1, F2}$
DMSO	10	2.10±0.21$^{C1, D1}$	504.69±180.56$^{A2, D1, E2, F2}$	251±72$^{A1, B3, E2}$	4.22±0.74^{C1}

Table 2
Biochemical Parameters Measured in Brain Tissue. This table presents the levels of BCL-2, Cyt-C, CAPN1, TNF-a, Caspase-3, MDA, and CAT in brain tissue samples from different groups (n=7). The data are presented as mean ± S.D. in each group. Significant differences ($p<0.05$) were observed between the Control and I/R, CuO-NP, CuO-NP+I/R, I/R+ALLN, and CuO-NP+ALLN groups, as indicated by the corresponding letters (A-F) and numbers (1−3). Specifically, the numbers 1, 2, and 3 indicate p-values of less than 0.001, 0.01, and 0.05, respectively.

Groups	N	BCL-2 (nmol/mg pro)	Cyt-C (ng/mg pro)	CAPN1 (ng/mg pro)	TNF-α (pg/mg pro)	Caspase-3 (ng/mg pro)	MDA (nmol/mg pro)	CAT (μmol/mg pro)
Control	7	0.10±0.02	0.64±0.07	0.16±0.02	617.10±133	3.54±0.18	5.41±0.28	0.87±0.13
I/R	7	0.07±0.01^{A2}	0.88±0.08^{A3}	0.27±0.04	673.90±52	4.55±0.46^{A2}	6.71±0.60^{A3}	0.74±0.05$^{, A3}$
CuO-NP	7	0.06±0.02^{A2}	1.12±0.08^{A1}	0.33±0.05^{A2,}	849.59±69$^{A2, B3}$	5.13±0.18^{A1}	7.37±0.26^{A1}	0.71±0.08^{A2}
CuO-NP+I/R	7	0.05±0.01^{A1}	1.29±0.02$^{A1, B2}$	0.44±0.05$^{A1, B2}$	1053.82±27$^{A1, B1}$	5.08±0.56^{A1}	7.87±0.01$^{A1, B2}$	0.69±0.06^{A2}
I/R+ALLN	7	0.07±0.03^{A3}	0.79±0.07$^{C2, D2}$	0.22±0.03^{D2}	613.93±52$^{C1, D1}$	4.01±0.50$^{C2, D2}$	6.26±0.49$^{C2, D1}$	0.84±0.08$^{C2, D2}$
CuO-NP+ALLN	7	0.08±0.02^{E2}	0.98±0.22$^{A2, D3}$	0.25±0.14^{D2}	56486±106$^{C2, D1}$	4.92±0.15$^{A1, E3}$	7.12±0.07$^{A1, E1}$	0.83±0.09$^{C3, D2}$
CuO-NP+I/R+ALLN	7	0.10±0.01$^{B2, C1, D1, E2, F3}$	0.69±0.26$^{C2, D1, F3,}$	0.27±0.10^{E1}	813.50±41$^{A3, E2, F2}$	4.64±0.54^{A2}	6.73±0.47$^{A2, D2}$	0.88±0.12$^{B3, C2, D2}$
DMSO	7	0.08±0.02$^{C2, D2}$	0.76±0.27$^{C2, D1}$	0.18±0.08$^{C3, D2}$	807.42±115$^{A3, E2,F2}$	3.64±0.27$^{B3, C1, D1, F2}$	6.45±0.16$^{C3, D1, F3}$	0.81±0.05$^{C3, D3}$

extensively studied in the literature and have been found to be useful indicators of traumatic and ischemic brain injury. Although NSE is commonly considered a definitive biomarker of neuronal damage, some studies have reported conflicting results due to its presence in red blood cells and platelets. Our study found that NSE levels were elevated after I/R and CuO-NP exposure, but treatment with ALLN significantly reduced NSE levels [34–36,41,42]. An increase in NSE levels has been observed after multiple traumas, but this increase is not specific to brain cell injury formation. As a result, its usefulness as a differential marker for measuring the extent of brain injury is limited. Our study found that NSE levels were higher after I/R and CuO-NP exposure, but the high NSE levels were significantly reduced in the groups treated with ALLN [34, 36,41,42].

5. Conclusion

The fact of that calpain and caspases were activated more after I/R and CuO-NP exposure in our animal model shows that brain cells were damaged. In rats, we saw an increase in apoptotic neuronal death signals at the same time as an increase in calpain and caspase after they were exposed to CuO-NP and had an I/R injury. Our findings show that the calpain inhibitor used for treatment might have a protective effect, as shown by the lower levels of apoptosis after I/R and CuO-NP exposure. This leads us to conclude that the calpain inhibitor may have a protective effect in different severity levels of damage, as indicated by the apoptotic results. TNF-α levels, a pro-inflammatory cytokine measured after I/R and CuO-NP exposure, showed significant changes in various groups. In our study, brain damage had an impact on the activity of free oxygen radicals and lipid peroxides, which are involved in activating the chemotaxis of neutrophils. ALLN positively affected the changing ROS values. Our study used MBP, NEFL, NSE, and B (S100), which have various intracellular and extracellular regulatory activities, as markers of neuronal damage. Significant differences were found in these four markers before and after treatment. The levels of cytochrome C, a protein in the mitochondrial membrane that plays a part in cell death signaling pathways inside mitochondria, showed that I/R and CuO-NP exposure damaged the mitochondrial membrane. The inhibition of proteases may protect axons, neurons, and glia, making it a potential therapeutic target for preventing brain cell damage. Our research has found that increased calpain is crucial in causing apoptotic cell damage in rats and brain models exposed to CuO-NP. Understanding when and how cells die in the brain after ischemia through necrosis and apoptosis has helped us show that calpain inhibitor-I (ALLN) can stop brain cells from dying permanently and could be used as a treatment. In conclusion, ALLN has the potential to be a valuable substance for preventing brain damage and could contribute to future studies on cell damage in the human brain.

Compliance with Ethical Standards

We confirm that all methods used in this study involving animal subjects were carried out in accordance with relevant guidelines and regulations. The Istanbul Medipol University Institutional Animal Ethics Committee, which is in charge of ensuring compliance with international standards and regulations, approved the animal handling protocol. The authorization number for this study was 38828770–604.01.01-E.15939.

Funding

This study was funded by TÜBİTAK (The Scientific and Technological Research Council of Turkey) under program code 3001 and project number 216S985.

Declaration of Competing Interest

The authors declare the following financial interests/personal relationships which may be considered as potential competing interests: Hadi KARIMKHANI reports financial support was provided by TUBITAK Informatics and Information Security Research Center. Hadi KARIMKHANI reports a relationship with TUBITAK Informatics and Information Security Research Center that includes: funding grants. The authors declare that they have no conflict of interest. If there are other authors, they declare that they have no known competing financial interests or personal relationships that could have appeared to influence the work reported in this paper

References

[1] I. Harukuni, A. Bhardwaj, Mechanisms of Brain Injury after Global Cerebral Ischemia, Neurol. Clin. 24 (2006) 1–21, https://doi.org/10.1016/j.ncl.2005.10.004.

[2] J. Shang, J. Jiao, M. Yan, J. Wang, Q. Li, L. Shabuerjiang, Y. Lu, Q. Song, L. Bi, G. Huang, X. Zhang, Y. Wen, Y. Cui, K. Wu, G. Li, P. Wang, X. Liu, Chrysin protects against cerebral ischemia-reperfusion injury in hippocampus via restraining oxidative stress and transition elements, Biomed. Pharmacother. 161 (2023) 114534, https://doi.org/10.1016/j.biopha.2023.114534.

[3] H. de Groot, U. Rauen, Ischemia-reperfusion injury: processes in pathogenetic networks: a review, Transplant. Proc. 39 (2007) 481–484, https://doi.org/10.1016/j.transproceed.2006.12.012.

[4] R.O.S. Soares, D.M. Losada, M.C. Jordani, P. Évora, O. Castro-e-Silva, Ischemia/Reperfusion Injury Revisited: An Overview of the Latest Pharmacological Strategies, Int. J. Mol. Sci. 20 (2019) 5034, https://doi.org/10.3390/ijms20205034.

[5] B. Miller, J.C.-T.J. of physiology, undefined 2016, TRPM2 protects against tissue damage following oxidative stress and ischaemia–reperfusion, Wiley Online Libr. Miller, JY CheungThe J. Physiol. 2016•Wiley Online Libr. 594 (2016) 4181–4191. https://doi.org/10.1113/JP270934.

[6] S.A. Saeed, K.F. Shad, T. Saleem, F. Javed, M.U. Khan, Some new prospects in the understanding of the molecular basis of the pathogenesis of stroke, Exp. Brain Res. 182 (2007) 1–10, https://doi.org/10.1007/s00221-007-1050-9.

[7] P. Lipton, Ischemic Cell Death in Brain Neurons, Physiol. Rev. 79 (1999) 1431–1568, https://doi.org/10.1152/physrev.1999.79.4.1431.

[8] T.V.P. Bliss, G.L. Collingridge, A synaptic model of memory: long-term potentiation in the hippocampus, Nature 361 (1993) 31–39, https://doi.org/10.1038/361031a0.

[9] K. Saravanakumar, A. Sathiyaseelan, A.V.A. Mariadoss, H. Xiaowen, M.H. Wang, Physical and bioactivities of biopolymeric films incorporated with cellulose, sodium alginate and copper oxide nanoparticles for food packaging application, Int. J. Biol. Macromol. 153 (2020) 207–214, https://doi.org/10.1016/J.IJBIOMAC.2020.02.250.

[10] M. Mesgari, A.H. Aalami, T. Sathyapalan, A. Sahebkar, A comprehensive review of the development of carbohydrate macromolecules and copper oxide nanocomposite films in food nanopackaging, Bioinorg. Chem. Appl. 2022 (2022), https://doi.org/10.1155/2022/7557825.

[11] M. Vats, S. Bhardwaj, A. Chhabra, Green Synthesis of Copper Oxide Nanoparticles using Cucumis sativus (Cucumber) Extracts and their Bio-Physical and Biochemical Characterization for Cosmetic and Dermatologic Applications, Endocr. Metab. Immune Disord. Drug Targets 21 (2021) 726–733, https://doi.org/10.2174/1871530320666200705212107.

[12] S. Pan, T.B. Goudoulas, J. Jeevanandam, K.X. Tan, S. Chowdhury, M.K. Danquah, Therapeutic applications of metal and metal-oxide nanoparticles: dermato-cosmetic perspectives, Front. Bioeng. Biotechnol. 9 (2021) 724499, https://doi.org/10.3389/fbioe.2021.724499.

[13] S.-L. Liao, W.-Y. Chen, S.-L. Raung, J.-S. Kuo, C.-J. Chen, Association of immune responses and ischemic brain infarction in rat, Neuroreport 12 (2001) 1943–1947, https://doi.org/10.1097/00001756-200107030-00034.

[14] H.L. Karlsson, P. Cronholm, J. Gustafsson, L. Möller, Copper oxide nanoparticles are highly toxic: a comparison between metal oxide nanoparticles and carbon nanotubes, Chem. Res. Toxicol. 21 (2008) 1726–1732, https://doi.org/10.1021/tx800064j.

[15] Y. Wang, Y. Liu, X. Bi, M. Baudry, Calpain-1 and Calpain-2 in the Brain: New Evidence for a Critical Role of Calpain-2 in Neuronal Death, Cells 9 (2020) 2698, https://doi.org/10.3390/cells9122698.

[16] M. Sato, E. Tani, T. Matsumoto, H. Fujikawa, S. Imajoh-Ohmi, Generation of the catalytic fragment of protein kinase C alpha in spastic canine basilar artery, J. Neurosurg. 87 (1997) 752–756, https://doi.org/10.3171/jns.1997.87.5.0752.

[17] N.I. Marín-Ramos, M. Pérez-Hernández, A. Tam, S.D. Swenson, H.-Y. Cho, T. Z. Thein, F.M. Hofman, T.C. Chen, Inhibition of motility by NEO100 through the calpain-1/RhoA pathway, J. Neurosurg. 133 (2020) 1020–1031, https://doi.org/10.3171/2019.5.JNS19798.

[18] R.C. Knopp, A. Jastaniah, O. Dubrovskyi, I. Gaisina, L. Tai, G.R.J. Thatcher, Extending the calpain–cathepsin hypothesis to the neurovasculature: protection of brain endothelial cells and mice from neurotrauma, ACS Pharmacol. Transl. Sci. 4 (2021) 372–385, https://doi.org/10.1021/acsptsci.0c00217.

[19] A.O. Ilhan, M. Ozkoc, K.K. Ol, H. Karimkhani, H. Senturk, D. Burukoglu, G. Kanbak, Protective effect of betaine against skeleton muscle apoptosis in rats induced by chronic alcohol and statin consumption, Bratisl. Med. J. 121 (2020) 589–599, https://doi.org/10.4149/BLL_2020_098.

[20] P. Syntichaki, N. Tavernarakis, The biochemistry of neuronal necrosis: rogue biology? Nat. Rev. Neurosci. 4 (2003) 672–684, https://doi.org/10.1038/nrn1174.

[21] T. Dalkara, E. Morikawa, N. Panahian, M.A. Moskowitz, Blood flow-dependent functional recovery in a rat model of focal cerebral ischemia, Am. J. Physiol. Circ. Physiol. 267 (1994) H678–H683, https://doi.org/10.1152/ajpheart.1994.267.2.H678.

[22] E. El Eter, A. Al Tuwaijiri, H. Hagar, M. Arafa, In vivo and in vitro antioxidant activity of ghrelin: Attenuation of gastric ischemic injury in the rat, J. Gastroenterol. Hepatol. 22 (2007) 1791–1799, https://doi.org/10.1111/j.1440-1746.2006.04696.x.

[23] J. Hu, L. Chen, X. Huang, K. Wu, S. Ding, W. Wang, B. Wang, C. Smith, C. Ren, H. Ni, Q. ZhuGe, J. Yang, Calpain inhibitor MDL28170 improves the transplantation-mediated therapeutic effect of bone marrow-derived mesenchymal stem cells following traumatic brain injury, Stem Cell Res. Ther. 10 (2019) 96, https://doi.org/10.1186/s13287-019-1210-4.

[24] R. Lei, C. Wu, B. Yang, H. Ma, C. Shi, Q. Wang, Q. Wang, Y. Yuan, M. Liao, Integrated metabolomic analysis of the nano-sized copper particle-induced hepatotoxicity and nephrotoxicity in rats: A rapid in vivo screening method for nanotoxicity, Toxicol. Appl. Pharmacol. 232 (2008) 292–301, https://doi.org/10.1016/j.taap.2008.06.026.

[25] D.P. Singh, K. Chopra, Verapamil augments the neuroprotectant action of berberine in rat model of transient global cerebral ischemia, Eur. J. Pharmacol. 720 (2013) 98–106, https://doi.org/10.1016/j.ejphar.2013.10.043.

[26] S. Cuzzocrea, M.C. McDonald, E. Mazzon, D. Siriwardena, I. Serraino, L. Dugo, D. Britti, G. Mazzullo, A.P. Caputi, C. Thiemermann, Calpain Inhibitor I Reduces the Development of Acute and Chronic Inflammation, Am. J. Pathol. 157 (2000) 2065–2079, https://doi.org/10.1016/S0002-9440(10)64845-6.

[27] Y. Yoshikawa, H. Hagihara, Y. Ohga, C. Nakajima-Takenaka, K. Murata, S. Taniguchi, M. Takaki, Calpain inhibitor-1 protects the rat heart from ischemia-reperfusion injury: analysis by mechanical work and energetics, Am. J. Physiol. Circ. Physiol. 288 (2005) H1690–H1698, https://doi.org/10.1152/ajpheart.00666.2004.

[28] Z.S. Ataizi, M. Ozkoc, G. Kanbak, H. Karimkhani, D. Burukoglu Donmez, N. Ustunisik, B. Ozturk, Evaluation of the neuroprotective role of boric acid in preventing traumatic brain injury-mediated oxidative stress, Turk. Neurosurg. (2019), https://doi.org/10.5137/1019-5149.JTN.25692-18.5.

[29] A.W. Smith, A. Das, M.K. Guyton, S.K. Ray, B. Rohrer, N.L. Banik, Calpain Inhibition Attenuates Apoptosis of Retinal Ganglion Cells in Acute Optic Neuritis, Investig. Opthalmol. Vis. Sci. 52 (2011) 4935, https://doi.org/10.1167/iovs.10-7027.

[30] A. Das, E.A. Sribnick, J.M. Wingrave, A.M. Del Re, J.J. Woodward, S.H. Appel, N. L. Banik, S.K. Ray, Calpain activation in apoptosis of ventral spinal cord 4.1 (VSC4.1) motoneurons exposed to glutamate: Calpain inhibition provides functional neuroprotection, J. Neurosci. Res. 81 (2005) 551–562, https://doi.org/10.1002/jnr.20581.

[31] A. Das, M.K. Guyton, D.D. Matzelle, S.K. Ray, N.L. Banik, Time-dependent increases in protease activities for neuronal apoptosis in spinal cords of Lewis rats during development of acute experimental autoimmune encephalomyelitis, J. Neurosci. Res. 86 (2008) 2992–3001, https://doi.org/10.1002/jnr.21737.

[32] H. Karimkhani, M. Özkoç, P. Shojaolsadati, K. Uzuner, D.B. Donmez, G. Kanbak, Protective Effect of Boric Acid and Omega-3 on Myocardial Infarction in an Experimental Rat Model, Biol. Trace Elem. Res. 199 (2021) 2612–2620, https://doi.org/10.1007/s12011-020-02360-z.

[33] S. Pugazhenthi, A. Nesterova, P. Jambal, G. Audesirk, M. Kern, L. Cabell, E. Eves, M.R. Rosner, L.M. Boxer, J.E.B. Reusch, Oxidative stress-mediated down-regulation of bcl-2 promoter in hippocampal neurons, J, Neurochem 84 (2003) 982–996. ⟨https://doi.org/10.1046/j.1471-4159.2003.01606.x⟩.

[34] R. Donato, G. Sorci, F. Riuzzi, C. Arcuri, R. Bianchi, F. Brozzi, C. Tubaro, I. Giambanco, S100B's double life: Intracellular regulator and extracellular signal, Biochim. Biophys. Acta - Mol. Cell Res. 1793 (2009) 1008–1022, https://doi.org/10.1016/j.bbamcr.2008.11.009.

[35] R.P. Berger, P.D. Adelson, M.C. Pierce, T. Dulani, L.D. Cassidy, P.M. Kochanek, Serum neuron-specific enolase, S100B, and myelin basic protein concentrations after inflicted and noninflicted traumatic brain injury in children, J. Neurosurg. Pediatr. 103 (2005) 61–68, https://doi.org/10.3171/ped.2005.103.1.0061.

[36] R.P. Berger, T. Dulani, P.D. Adelson, J.M. Leventhal, R. Richichi, P.M. Kochanek, Identification of Inflicted Traumatic Brain Injury in Well-Appearing Infants Using Serum and Cerebrospinal Markers: A Possible Screening Tool, Pediatrics 117 (2006) 325–332, https://doi.org/10.1542/peds.2005-0711.

[37] M.M. Gresle, H. Butzkueven, G. Shaw, Neurofilament Proteins as Body Fluid Biomarkers of Neurodegeneration in Multiple Sclerosis, Mult. Scler. Int. 2011 (2011) 1–7, https://doi.org/10.1155/2011/315406.

[38] J. Aronowski, K.-H. Cho, R. Strong, J.C. Grotta, Neurofilament Proteolysis after Focal Ischemia; When Do Cells Die after Experimental Stroke? J. Cereb. Blood Flow. Metab. 19 (1999) 652–660, https://doi.org/10.1097/00004647-199906000-00008.

[39] M. Kobek, Z. Jankowski, J. Szala, Z. Gąszczyk-Ożarowski, A. Pałasz, R. Skowronek, Time-related morphometric studies of neurofilaments in brain contusions, Folia Neuropathol. 1 (2016) 50–58, https://doi.org/10.5114/fn.2016.58915.

[40] M. Özkoç, H. Karimkhani, G. Kanbak, D. Burukoğlu Dönmez, Hepatotoxicity and nephrotoxicity following long-term prenatal exposure of paracetamol in the

neonatal rat: is betaine protective? Turk. J. Biochem. 45 (2020) 99–107, https://doi.org/10.1515/tjb-2018-0307.

[41] L.E. Pelinka, H. Hertz, W. Mauritz, N. Harada, M. Jafarmadar, M. Albrecht, H. Redl, S. Bahrami, Nonspecific Increase Of Systemic Neuron-Specific Enolase After Trauma: Clinical And Experimental Findings, Shock 24 (2005) 119–123, https://doi.org/10.1097/01.shk.0000168876.68154.43.

[42] Z. Zhang, S. Mondello, F. Kobeissy, R. Rubenstein, J. Streeter, R.L. Hayes, K.K. W. Wang, Protein biomarkers for traumatic and ischemic brain injury: from bench to bedside, Transl. Stroke Res. 2 (2011) 455–462, https://doi.org/10.1007/s12975-011-0137-6.